

Synthesis, Stereochemistry, and Spin Transition of Heterometal Dinuclear Fe(II)–Cr(III) Complex Bridged by 3,5-Bis(pyridin-2-yl)-pyrazolate

Keiko Ni-iya, Akira Fuyuhiro, Takashi Yagi, Saburo Nasu,† Kaori Kuzushita,† Syotaro Morimoto,† and Sumio Kaizaki*

Department of Chemistry, Graduate School of Science, Osaka University, Toyonaka, Osaka, 560-0043

†Department of Physical Science, Graduate School of Engineering Science, Osaka University, Toyonaka, Osaka, 560-8531

(Received May 14, 2001)

We have synthesized and characterized a new heterometal dinuclear complex, [(nta)Cr^{III}(μ-bpypz)Fe^{II}(picen)]BF_4 (**1**), where nta = nitritotriacetate; bpypz$^-$ =3,5-bis(pyridin-2-yl)-pyrazolate; and picen = *N*,*N*′-bis-(2-pyridylmethyl)ethylenediamine. The X-ray structure of the Fe(II)–Cr(III)·H_2O·3dmf demonstrated that this has a dinuclear structure with a highly distorted octahedron around a high-spin Fe(II) and intramolecular bifurcated three-centered hydrogen bonds between the carboxylate oxygens of the nta and an amine proton of the picen with an abnormal conformation. A magnetic susceptibility measurement and/or the Mössbauer spectra of **1** substantiated a gradual spin-transition from 130 K to 300 K in a heating process centered around 250 K with a small hysteresis dip in the Fe(II) complex. The spin-transition temperature of **1** is lower than that of the mononuclear complex, [Fe^{II}(picen)(Hbpypz)]$(BF_4)_2$(**2**), resulting from the weaker ligand field of **1** with a distorted octahedron than that of **2**.

Since various kinds of Fe(II) complexes exhibit spin transitions between the high-spin(S = 2) and low-spin(S = 0) in terms of external perturbations, such as temperature, pressure and light, there have been a number of investigations concerning the spin crossover of Fe(II) complexes, which have been reviewed from various respective points of view.[1–6] More recently, growing attention to spin crossover phenomena has been paid in relation to molecular devices or switches.[7]

Although most interest has been focused on mononuclear Fe(II) complexes, an increasing number of examples for di- or polynuclear complexes have been reported, for which spin crossovers may be favorable for weak antiferromagnetic interactions between the high-spin states of Fe(II) and/or paramagnetic metal species.[7a,b] Spin crossover Fe(II) dinuclear complexes linked with a non-spin crossover paramagnetic luminous complex, such as the Cr(III) ion could be a suitable candidate for studying the influence of the photochemical or photophysical properties of luminophores on light-induced excited spin state trapping (LIESST)[8] as well as the effect of the magnetic interaction on spin crossover. Another expectation from dinuclear complexes is some steric effect on spin crossover phenomena by controlling or tuning the coordination environment in terms of the intramolecular interaction in dinuclear structures. Such stereochemical aspects have been demonstrated by our recent studies on the pyrazolate-3,5-dicarboxylate(pzdc) bridged dinuclear Cr(III) complexes; hydrogen bonds stabilize or entrap the unstable unsym-*cis* configuration and/or the abnormal conformation of the tetradentate ethylenediamine-*N*,*N*′-diacetate and its analogues.[9–10] This stereochemical requirement may also play important roles in relation to the dynamic spin crossover process. Thus, the design and synthesis of heterometal dinuclear Fe(II) complexes including a paramagnetic Cr(III) counter part could give invaluable hints to spin crossover in Fe(II)–Fe(II) di- and polynuclear complexes.[7,11–15]

In this paper, we report on the preparation and characterization of a new heterometal dinuclear Fe(II)–Cr(III) complex bridged by the bpypz$^-$ (3,5-bis(pyridin-2-yl)-pyrazolate) ligand. The spectroscopic and magnetic properties are examined in view of the spin crossover phenomenon.

Experimental

Materials. *N*,*N*′-bis(2-pyridylmethyl)ethylenediamine(picen)[16] and 3,5-bis(pyridin-2-yl)pyrazole(Hbpypz)[17] were obtained by literature methods. Nitritotriacetic acid (H_3nta) and 4,7,13,16,21,24-hexaoxa-1,10-diazabicyclo[8.8.8]hexacosane(cryptand[2.2.2]) were purchased from Wako Chemicals Co. and Aldrich Co., respectively.

Preparation of Complexes. [(nta)Cr(μ-bpypz)Fe(picen)]BF_4 (1). The synthesis was operated in a N_2 stream under an anaerobic condition. The preparation of the starting complex, [Cr(nta)(Hbpypz)]·$3H_2O$ (0.26 g, 0.5 mmol) (**3**), is described below. Complex **3** was dissolved in methanol (10 mL) by adding cryptand[2.2.2] (0.18 g, 0.5 mmol). To this solution was added $Fe(BF_4)_2$·$6H_2O$ (0.17 g, 0.5 mmol). Then, a pale-yellow powder was precipitated. To this mixture was added a methanol solution (3 mL) of picen (0.12 g, 0.5 mmol). After the mixture was stirred for one day at room temperature, a yellow-brown precipitate was obtained. This was filtered by suction as soon as possible and

washed with methanol, and dried. It was then recrystallized by a diffuse evaporation method in dimethylformamide(dmf) and ether. The obtained brown plates were identified as [(nta)Cr(μ-bpypz)Fe(picen)]BF_4·H_2O·3dmf by an X-ray analysis, but the elemental analysis indicated the hydrate, **1**·2.5H_2O, as follows. Found: C, 45.21; H, 4.15, N, 13.95%. Calcd for $CrFeC_{33}H_{38}N_9O_{8.5}BF_4$: C, 44.47; H, 4.30, N, 14.14%. This change of crystallization solvents resulted from the efflorescence and/or hygroscopic properties of brown crystals in air. Magnetic moment: μ_{eff} = 5.40 at 298 K

[Fe(picen)(Hbpypz)] (BF_4)$_2$·0.5(C_2H_5)$_2$O·2H_2O (2). To a methanol solution of picen (0.12 g, 0.5 mmol) was added 0.17 g (0.5 mmol) of Fe(BF_4)$_2$·6H_2O under a N_2 stream. The color of the solution turned to blue violet. To this solution was added 0.11 g (0.5 mmol) of Hbpypz in 5 mL of methanol. After stirring for 5 h, the solution changed to yellow-brown. A dark red precipitate was obtained when ether was added to this solution. The solid was filtered off immediately and washed with ether.

Found: C, 47.18; H. 4.68; N, 15.14%. Calcd for $FeC_{29}H_{33}N_8O_{2.5}B_2F_8$: C, 46.62; H, 4.45, N, 15.00%. Magnetic moment: μ_{eff} = 3.10 at 298 K.

[Cr(nta)(Hbpypz)]·3H_2O (3). The starting complex K[Cr(OH)(nta)(H_2O)] was prepared by a literature method.[18] K[Cr(OH)(nta)(H_2O)] (1.75 g, 5 mmol) was dissolved in 10 mL of water in a water bath. To this solution was added Hbpypz (1.11 g, 5 mmol) in 0.5 mL of concentrated HCl. During stirring, a red precipitate was obtained. This was filtered off and the powder was washed with methanol, and then dried in vacuo. Found: C, 43.68; H, 4.24; N, 13.49%. Calcd for $CrC_{19}H_{22}N_5O_9$: C, 44.19; H, 4.29, N, 13.56%.

The Deuterated Complexes. Deuterated picen-d_2(2-py-CHD_1-$NHCH_2CH_2NH$-CHD_1-2-py) was synthesized by using ethanol-d_1 (C_2H_5OD) and acetic acid-d_1(CH_3COOD).

A deuterated nta-d_6 complex, [Cr(nta-d_6)(Hbpypz)] (nta-d_6 = $N(CD_2COO^-)_3$), was obtained by crystallization after heating a solution of [Cr(nta)(Hbpypz)] in D_2O. [(nta- d_6)Cr(μ-bpypz)Fe(picen-d_2)]BF_3 was prepared by the same method as that for the all-proton one.

X-ray Analysis. A brown plate crystal of $C_{42}H_{56}O_{10}N_{12}CrFeBF_4$ having approximate dimensions of 0.20 × 0.20 × 0.10 mm was mounted in a glass capillary. An attempt to make an X-ray analysis by a four-circle diffractometer failed, since a crystal of **1**·H_2O·3dmf was decomposed during the measurement. On the other hand, all of the measurements were successfully made on a Rigaku RAXIS-RAPID Imaging Plate. The data were collected at a temperature of 23 ± 1 °C to a maximum 2θ value of 55.0°, 55 images corresponding to 220.0° oscillation angles with $\Delta\Omega$ = 4.0° step. The exposure time was 3.30 min per degree. Data were processed by the PROCESS-AUTO program package.

Of the 26915 reflections which were collected, 11060 were unique. A symmetry-related absorption correction using the program ABSCOR was applied, which resulted in transmission factors ranging from 0.58 to 0.94. The data were corrected for Lorentz and polarization effects.

Structure Solution and Refinement. The structure was solved by direct methods. Some non-hydrogen atoms were refined anisotropically, while the rest were refined isotropically. Hydrogen atoms were included, but not refined.

All calculations were performed using the teXsan crystallographic software package of Molecular Structure Corporation. Crystallographic data and selected bond distance and angles are listed in Tables 1 and 2.

Measurements. UV-vis spectra were obtained by a Perkin-Elmer Lambda 19 spectrophotometer. The variable temperature UV-vis spectra were measured using polystyrene films by the same spectrophotometer attached with an Oxford CF1204 cryostat. ^1H and ^2H NMR spectra were recorded by Jeol EX-270 and Jeol LAMBDA-500 spectrometers, respectively. The magnetic susceptibility of the powders was measured at 1000 Oe between 2–300 K by a MPMS-5S Quantum Design. Pascal's constants were used for diamagnetic corrections to determine the constituent atom diamagentism. The magnetic susceptibilities in solution were obtained by the Evans method, which was modified for a SCM FT-NMR spectrometer.[19] The measurements were carried out on a dmf-d_7 solution containing a 10.5 mmol dm^{-3} complex **1** and 2% *t*-butanol and 2% TMS as internal references. Negative ion ESI-Mass spectra were measured by a API-Lambda-500 Mass

Table 1. Crystallographic Data for [(nta)Cr(μ-bpypz)-Fe(picen)]BF_4·H_2O·3dmf

Chemical formula	$CrFeC_{33}H_{33}N_9O_6BF_4$·$H_2O$·3($C_3H_7NO$)
Formula weight	1083.63
Crystal color	brown
Crystal system	monoclinic
Space group	$P2_1/n$
a/Å	17.2614(9)
b/Å	15.9452(11)
c/Å	18.4754(13)
β/°	102.783(3)
V/Å^3	4959.1(6)
Z	4
D_{calcd}/Mg m^{-3}	1.451
λ	0.71073 Å
μ	5.9 cm^{-1}
Temperature	296.5 K
$R1$[a)]	0.0668
$wR2$[b)]	0.1591

a) $R1 = \Sigma||F_o|-|F_c||/\Sigma|F_o|$.
b) $wR2 = [(\Sigma w(|F_o|-|F_c|)^2/\Sigma wF_o^2)]^{1/2}$

Table 2. Selected Bond Lengths (Å) and Angles(°) of **1**·H_2O·3dmf

Cr–O1	1.935(4)	Fe–N1	2.244(5)
Cr–O3	1.972(4)	Fe–N2	2.171(6)
Cr–O5	1.959(4)	Fe–N3	2.190(5)
Cr–N5	2.074(5)	Fe–N4	2.243(6)
Cr–N8	2.017(5)	Fe–N6	2.202(5)
Cr–N9	2.124(5)	Fe–N7	2.168(4)
O1–Cr–O3	91.5(2)	N1–Fe–N2	80.4(2)
O1–Cr–O5	94.0(2)	N1–Fe–N3	73.7(2)
O1–Cr–N5	83.6(2)	N1–Fe–N4	102.9(2)
O1–Cr–N8	91.6(2)	N1–Fe–N6	94.3(2)
O1–Cr–N9	170.6(2)	N1–Fe–N7	161.9(2)
O3–Cr–O5	161.9(2)	N2–Fe–N3	99.0(2)
O3–Cr–N5	81.6(2)		
O3–Cr–N8	96.5(2)		
O3–Cr–N9	89.9(2)		
O5–Cr–N5	81.8(2)		

spectrometer. ^{57}Fe Mössbauer spectra was obtained by 925 MBq where ^{57}Co in Rh was used as a γ-ray source. The velocity scale is relative to α-Fe at 300 K. A WISSEL MA-260 velocity transducer and a data acquisition system utilized by a personal computer were operated in the constant-acceleration mode. Using a thin-foil approximation, the data were analyzed by the usual least-squares-fit routine.

Results and Discussion

Synthesis and Characterization of Complexes. Because of the sensitivity to air oxidation of iron(II) complexes, the reactions were performed in a N_2-purged atmosphere. The product obtained from the reaction of [Cr(nta)(Hbpypz)] with $Fe(BF_4)_2\cdot 6H_2O$ and picen in methanol indicates the chemical formula $[(nta)Cr(bpypz)Fe(picen)]BF_4$ (**1**). This chemical constitution as well as the dinuclear entity was confirmed by the ES-MS spectra. The intensity ratio of the observed peaks around m/z = 759 are consistent with the calculated isotopic distribution corresponding to $[(nta)Cr(bpypz)Fe(picen)]^+$.

The X-ray Structure of 1·H$_2$O·3dmf. The molecular structure of the X-ray analysis is shown in Fig. 1. This complex has a dinuclear structure in which Cr(III) and Fe(II) with 4.472(1) Å length are bridged by a bpypz ligand. The chromium(III) ion is coordinated by a tetradentate nitrilotriacetato and nitrogen donor atoms of pyridyl and pyrazolato of bpypz, producing an octahedral *mer*-$Cr(N)_3(O)_3$ geometry, whereas the iron(II) ion is surrounded by a picen with a symmetrical-*cis* configuration and a bpypz ligand, making a distorted $Fe(N)_6$ octahedron. The bond distances , bond angles and dihedral angles of the nta moiety around the Cr(III) ion in **1**·H$_2$O·3dmf (Table 2) are somewhat different from those reported for $[(nta)Cr(OH)_2M(L)_2]Cl\cdot nH_2O$ (M = Cr(III) and/or Co(III); L = tn, phen)[20] and $Cs_2[Cr_2(nta)_2(\mu\text{-}OH)_2]\cdot 4H_2O$.[21] The Cr–O(1) distance (1.935(4) Å) is shorter and the O(1)–Cr–N(5) angle (83.6(2)°) is smaller than the reported ones (1.951–1.964 Å and 84.0(3)–85.0°, respectively). The torsion angle in absolute value for Cr–N(5)–C(16)–C(15) (1.7(6)°) is much smaller than those found for the other nta complexes: (13.9(4)° for the tn complex and 17(1)° for the phen complex).[20] These structural characteristics may be correlated with the hydrogen bond between the carboxylate of the nta and the amine proton of the picen, as mentioned below.

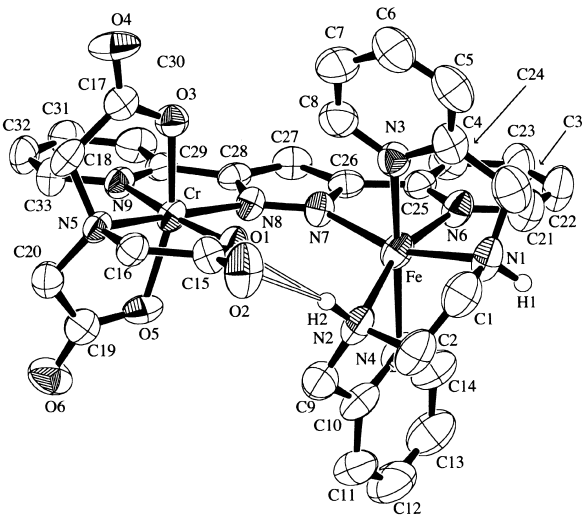

Fig. 1. ORTEP Drawing of complex **1**·H$_2$O·3dmf.

As shown in Fig. 1, an octahedron around the Fe(II) ion is highly distorted. In spite of the expected symmetrical *cis* configuration with a pseudo C_2 axis around the Fe(II) moiety, each aliphatic and aromatic amine–Fe(II) bond lengths are significantly different from each other. The Fe–N2 (2.171(6) Å) and Fe–N3 (2.190(5) Å) bond lengths are shorter than the corresponding Fe–N1 (2.244(5) Å) and Fe–N4 ones (2.243(6) Å), respectively. The N2–Fe–N7, N1–Fe–N4 and N1–Fe–N3 bond angles are 112.9(2)°, 102.9(2)° and 73.7(2)°, respectively, being larger and smaller by $|10°|$ than the regular octahedral values. This is in contrast to the case of $Na[Cr_2(\mu\text{-}pzdc)(edda)_2]\cdot 5H_2O$,[9] where only one bond angle exceeds +10° from the regular octahedral one. The stereochemical flexibility around the Fe(II) moiety results from the high-spin state of the Fe(II) ion, as inferred from the typical Fe–N bond lengths (2.16–2.24 Å). Moreover, it is noted that the ethylenediamine ring of the picen around the Fe(II) ion takes the abnormal *eq–eq*(N–C_{eq}) gauche conformation[22–23] with the torsion angle of N1–C1–C2–N2 being −58.4(7)°. In general, the abnormal conformation for the picen complexes and the analogues is less stable than the normal *ax–ax*(N–C_{ax}) one; only one example for the picen complex has been reported so far.[23] The overall absolute configuration for the Fe(II) moiety in **1** is designated as $\Delta(S_N,S_N;\lambda)$ and vice versa, where Δ, S_N and λ are the absolute configurations around the Fe(II) ion, the secondary amine and the conformation for the ethylenediamine ring, respectively. This deformed conformation could be entrapped within a pocket of the complex ligand $[(nta)Cr(bpypz)]^-$ and stabilized by the stereognostic interaction between the Cr(III) and Fe(II) moieties. That is, there are intramolecular hydrogen bonds between the proton of the secondary amine nitrogen , N2, of the picen and both of the coordinated carboxylate oxygen, O1, and uncoordinated one, O2, of nta as found for $Na[Cr_2(\mu\text{-}pzdc)(eddp)_2]\cdot 6H_2O$.[10] The bond distances from H2 to O1 and O2 are nearly equal to each other (2.263 Å and 2.274 Å), being within the range of the hydrogen-bond lengths. The angle sum around the hydrogen is α_1(N2–H2···O1) + α_2(N2–H2···O2) + α_3(O1···H2···O2) = 350.05°, and the H atom is close to the plane defined by N2, O1, and O2; Δ = 0.134 Å. These structural parameters range within the second or third frequent statistical distribution, demonstrating the three-center bifurcated hydrogen bond together with the asymmetric location of the hydrogen in the *syn* position with respect to the acceptor carboxylate oxygens.[10,24]

The pyrazolato moiety is mostly planar in view of the least-squares plane, but the shape is asymmetrically deformed; the C26–C27 bond lengths (1.410(8) Å) around pyrazolate of the bpypz is much longer than the C28–C27 one (1.373(8) Å) and the N8–C28–C27 bond angle (111.0(5) °) is larger than the N7–C26–C27 one (108.7(5) °).

The Cr–N8 and Fe–N7 bond lengths for the pyrazolate nitrogens are shorter, respectively, than the Cr–N9 and Fe–N6 ones for the pyridyl nitrogen, as found for the other bpypz complexes.[25] There has been found to be intermolecular stacking with a closest distance of 3.565(8) Å (min.) between the pyridyl planes of each bpypz moiety belonging to the other

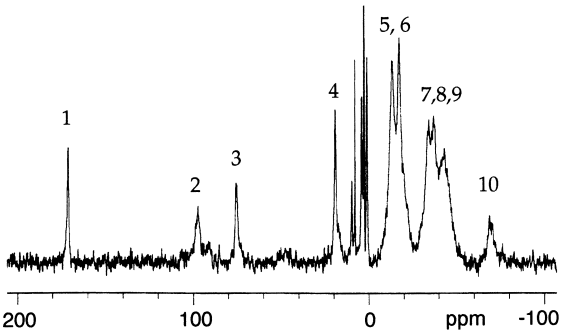

Fig. 2. ^{2}H NMR spectra of [(nta-d_6)Cr(μ-bpypz)Fe(picen-d_2)]$^-$ complex in dmf-d_7 at 288 K.

complex cations in complex **1**, as found for the analogous bpypz complexes.[25]

Solution Structure. The structure of **1** was confirmed to be retained in solution similarly to that in the crystals by the paramagnetic ^{2}H NMR spectra for both the deuterated (picen-d_2)Fe(II) and (nta-d_6)Cr(III) moieties as shown in Fig. 2. Four ^{2}H NMR signals (1–4 numbered in Fig. 2) down field (10–180 ppm) of the Fe(picen-d_2) moiety are observed in contrast to two signals for *sym-cis*-[Fe(NCS)$_2$(picen-d_2)], indicating the inequivalence of four methylene deuterons or two pyridyl methyl group in spite of the *sym-cis* configuration. This observation is consistent with the highly distorted octahedron around Fe(II), as described above concerning the crystal structure. Moreover, the ^{2}H NMR spectra for the deuterated nta complex gave six signals (5–10 numbered in Fig. 2) at a higher field (0–$-$80 ppm). In general, only three ^{2}H NMR signals were observed for nta-d_6Cr(III) complexes.[20,26] Therefore, three inequivalent methylenes inferred from six signals would result from the deformed conformation of the acetate chelate rings in the nta moiety, as suggested from the X-ray structure.

Magnetic Properties. The $\chi_M{\cdot}T$ value of **1**·2.5H$_2$O in the powder state is 3.81 emu mol^{-1} K at 330 K, which is smaller than that (4.877 emu mol^{-1} K) expected for a species consisting of 100% of the high spin Fe(II) (3.001 emu mol^{-1} K) and Cr(III) (1.876 emu mol^{-1} K). As shown in Fig. 3, the $\chi_M{\cdot}T$ values of **1**·2.5H$_2$O decrease gradually with lowering the temperature and they then remain mostly constant below 120 to 10 K (2.45–2.30 emu mol^{-1} K), followed by fairly decreasing to 2.20 emu mol^{-1} K at 4 K. The temperature dependence of the $\chi_M{\cdot}T$ values is reversible in both the cooling and warming modes, aside from a small hysteresis dip centered around 250 K in the heating mode. Assuming 100% low-spin Fe(II) and Cr(III) below 120 K, the $\chi_M{\cdot}T$ value should be close to that only for the Cr(III) moiety. However, the observed $\chi_M{\cdot}T$ value (2.40 emu mol^{-1} K) is larger than the expected one, suggesting the existence of a residual high-spin Fe(II) complex. This is confirmed by the Mössbauer spectra. The relative intensity ratio of the singlet peak and the doublet peaks, respectively, corresponding to the low-spin and high-spin Fe(II) complex clearly change from 298 K to 77 K, as in Fig. 4. An analysis by means of the least squares-fit routine of the Mössbauer spectra of complex **1** indicated that the high-spin Fe(II) complex decreases from 73% to 37% with lowering the temperature where the isomer shift changes from δ_{iso} 0.966 to 1.12 mm s^{-1} with a quadrupole splitting of ΔEq = 2.08 to 2.85 mm s^{-1} for the

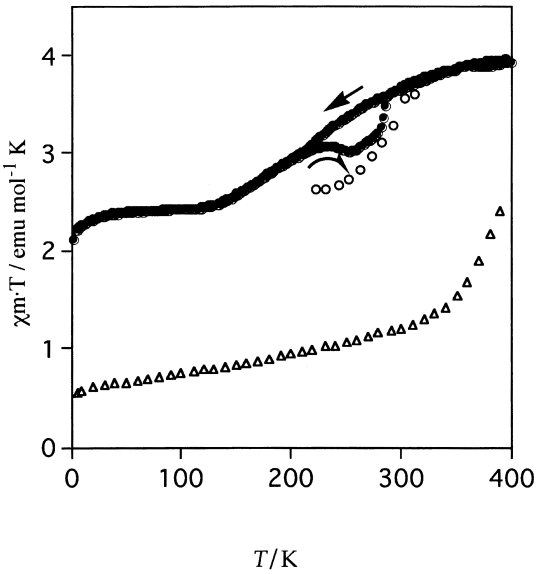

Fig. 3. A plot of the product of the magnetic susceptibility and temperature versus temperature. **1**·2.5H$_2$O: solid (●●●); dmf solution (○○○), **2**·0.5(C$_2$H$_5$)$_2$O·2H$_2$O: solid(△△△).

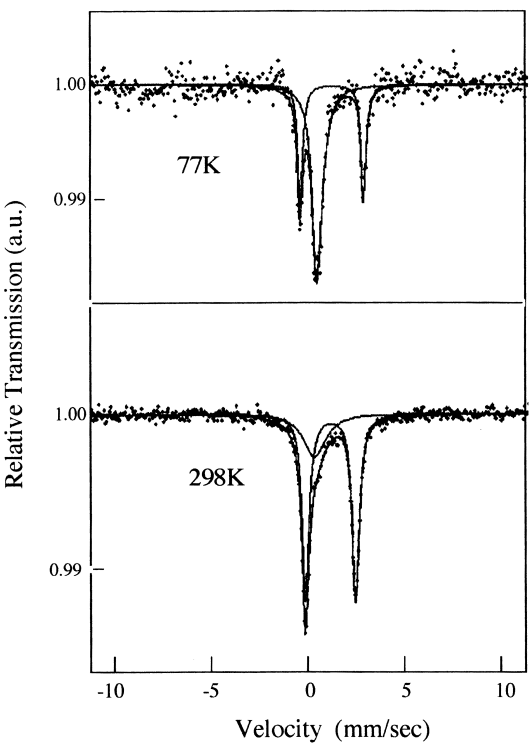

Fig. 4. Mössbauer spectra of **1**·2.5H$_2$O at 298 K (below) and 70 K (above).

high-spin case and from δ_{iso} 0.282 to 0.486 mm s^{-1} for low-spin. This fact indicates that the decrease in the $\chi_M{\cdot}T$ values arises mainly from the spin transition in the Fe(II) complex, in which the amount of the low-spin Fe(II) complex increases at the expense of a decrease in the high-spin one with lowering temperature; however, this is not solely due to the antiferromagnetic interaction between the paramagnetic Cr(III) and

high-spin Fe(II) complexes. The observed $\chi_M \cdot T$ values (ca. 2.4 emu mol^{-1} K) are smaller by ca. 0.49 emu mol^{-1} K than those (2.99 emu mol^{-1} K) estimated based on the high-spin ratio from the Mössbauer spectra. This reduction may be due to some antiferromagnetic interaction between the paramagnetic Cr(III) and the residual high-spin Fe(II) in complex **1**·2.5H_2O at low temperature. The spin transition temperature, T_c (ca. 250 K), of this dinuclear complex **1**·2.5H_2O is found to be lower than that (~400 K) of the mononuclear complex, [Fe(picen)(Hbpypz)]$(BF_4)_2$, **2**·0.5$(C_2H_5)_2O$·2H_2O. It is likely that this lowering of T_c results from the weaker ligand field in **1** due to the highly distorted coordination than that in the mononuclear one **2**. The π stacking in the solid, as found for the X-ray analysis, seems to be responsible for the cooperativity or the observed hysteresis, though the sample **1**·2.5H_2O for the SQUID measurement is not adventitiously identical with that of **1**·H_2O·3dmf for the X-ray analysis. From the magnetic susceptibilities measured by the Evans method[19] (Fig. 3), the spin transition in the solution is found to be less gradual, or more abrupt, than in the solid and the low-spin state in solution remains at a higher temperature than in the solid. This is contrary to the general tendency attributable to the crystal-packing effect, or cooperativity.[6]

UV-vis Absorption and Luminescence Spectra. The UV-vis spectra of **1**, **2** and **3** are shown in Fig. 5. The absorption maximum at 18,740 cm^{-1} of the mononuclear Cr(III) complex **3** is due to the first $^4A_2$–$^4T_2$ d–d ligand field transition, which is close to that (18,500 cm^{-1})[27] of the analogous type of complex, [Cr(nta)(phen)] (phen = 1,10-phenanthroline), with a *mer*-[CrO_3N_3] chromophore. Complexes **1** and **2** exhibit two intense MLCT bands near 17,200 and 23,000 cm^{-1}, which obscured the d–d bands. As a rule, the former low frequency band may be the MLCT from Fe(II) to the pyridyl imine chelates (e.g., bpypz), as observed for low-spin [Fe(6-Me-py)$_n$(py)$_{3-n}$tren]$^{2+}$ (n = 0–3)[28] and the latter high-frequency one to the low-spin poly(pyridylmethyl)alkylamine (e.g., picen) Fe(II) complexes.[6,8] For complex **1**, the intensity of the lower frequency band is stronger than that of the higher frequency band, in contrast to the case of complex **2**, which gives a comparable intensity, as shown in Fig. 5. The relative low MLCT intensity at 17,200 cm^{-1} in **1** may result from a change in the bpypz chromophore from **2** with the dangling protonated part (Hbpypz) to **1** with the coordinated Cr(III) unit (Cr-bpypz), but is not due simply to a smaller amount of the low-spin species for **1**, as compared with that for **2**, since the relative intensities of the two bands remain almost unchanged from 300 K to 7 K, as can be seen in Fig. 6. Another MLCT band attributed from the bpypz moiety shifts from 19,000 cm^{-1} in **2** to 20,000 cm^{-1} in **1**. This would also be related to the bpypz moiety. It is noted that the 23,000 cm^{-1} MLCT from Fe(II) to the picen moiety in **1** and **2** are not so much different from each other, even though the picen around Fe(II) in **1** is

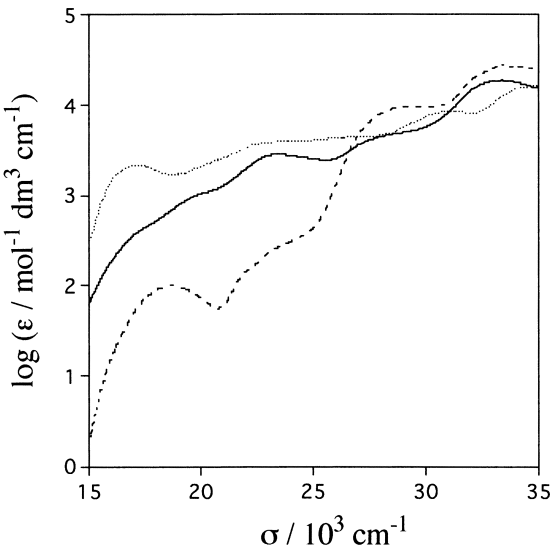

Fig. 5. UV-vis spectra of **1** (——), **2** (·····), **3** (------) in dmf at room temperature.

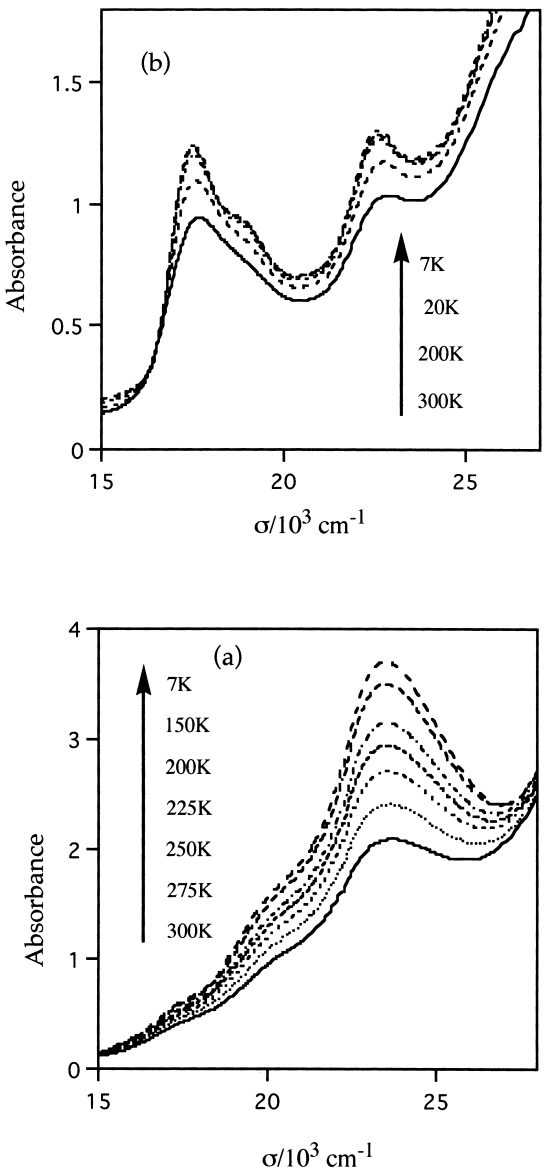

Fig. 6. Variable temperature UV-vis spectra of **1**·2.5H_2O (a) and **2**·0.5$(C_2H_5)_2O$·2H_2O (b) in polystyrene films, showing the intensity increase with lowering temperature according to the arrows.

highly distorted as mentioned above. Fig. 6 also shows that the MLCT band intensities around 17,200–20,000 and 23,000 cm^{-1} of complex **1** as well as **2** increase with lowering the temperature, indicating an increase of an low-spin complex, as expected from the observed $\chi_M \cdot T$ values (described above), leading to the spin equilibrium.

The luminescence around 100 K was not observed in the region of the $^2E \rightarrow {}^4A_2$ phosphorescence, characteristic for the Cr(III) moiety in the dinuclear Cr(III)–Fe(II) complex **1** with irradiation by a 514.5 nm laser, whereas the strong luminescence for the mononuclear complex **3**, having a similar chromophore to the Cr(III) moiety in complex **1**, was observed at 12,300 cm^{-1} under the same condition. The observed $^2E \rightarrow {}^4A_2$ luminescence peak of **3** is close to the $^5T_2 \rightarrow {}^5E$ transition of the high-spin Fe(II) complex, but higher than the lowest lying $^1A_1 \rightarrow {}^3T_1$ transition of the low-spin one. Thus, the complete quenching of the ^2E(Cr(III)) in **1** may result from energy transfer from the ^2E(Cr(III)) to $^3T_1$(low-spin Fe(II)) and/or ^5E (high-spin Fe(II)). If the ^2E(Cr(III)) state is located at lower energy than the ^5E(high-spin Fe(II)), the reverse LIESST[8] could occur by excitation with the lower frequency light for the $^4A_2 \rightarrow {}^2E$(Cr(III)) transition energy than the corresponding $^5T_2 \rightarrow {}^5E$ excitation energy usually used. At present, unfortunately, there is no indication for the LIESST or reverse LIESST[8] based on a comparison between the room temperature and 97 K Raman spectra, which are expected to provide a direct observation of such light-induced spin transitions.[29]

Conclusions

As expected for the pzdc[9,10] or bpypz bridged dinuclear complexes, the unstable or nonexistent abnormal conformation of the picen as well as the highly deformed octahedron in Fe(II) of complex **1** results from the intramolecular three-center bifurcated hydrogen bond, which is forced to capture the Fe(picen) unit within a pocket of the complex ligand, $[(nta)Cr(bpypz)]^-$. It is likely that this stereochemical peculiarity gives rise to the lowering of the spin transition temperature, as compared with that of the mononulcear complex **2**. It should be noted that the severe strained conformation of the picen around the high-spin Fe(II) moiety is retained with stability in the low-spin state during reversible structural changes from high-spin to low-spin complexes, and vice versa, associated with the dynamic process. This provides a clue to explore how the electronic properties or spin crossover phenomena are influenced by the structural modification under such unfamiliar conditions as entrapped conformations leading to deformed octahedral coordination. This type of complex will also promise to exhibit a light-induced excited pair spin state (e.g., high-spin $d^6(Fe^{II})$–$d^3(Cr^{III})$ pair with antiferromagnetically coupled S = 1/2) after the LIESST below T_c, as recently found for the homometal Fe(II) dinuclear complex.[15b] Further study on the related type of dinuclear Fe(II)–Co(III) and Fe(II)–Fe(II) complexes besides the LIESST and reverse LIESST experiments of complex **1** is in progress at our laboratory.

We acknowledge support of this research by a Grant-in-Aid for Scientific Research (No.10304056) and for Scientific Research on Priority Areas "Metal-assembled Complexes" (No.11136228) from the Ministry of Education, Science, Sports and Culture.

References

1 R. L. Martin and A. H. White, *Transition Met. Chem.*, **4**, 113 (1968).
2 H. A. Goodwin, *Coord. Chem. Rev.*, **18**, 293 (1976).
3 P. Gütlich, *Struct. Bonding*, **44**, 83 (1981).
4 E. König, G. Ritter, and S. K. Kulshreshtha, *Chem. Rev.*, **85**, 219 (1985).
5 E. König, *Adv. Inorg. Chem.*, **35**, 527 (1987).
6 H. Toflund, *Coord. Chem. Rev.*, **94**, 67 (1989).
7 a) J. Zarembowitch and O. Kahn, *New J. Chem.*, **15**, 181 (1991). b) H. Toflund, in "Magnetism: A Supramolecular Function," ed. by O. Kahn, Netherland, Kluwer Academic (1996), p.323. c) O. Kahn and C. J. Martinez, *Science*, **279**, 44 (1998). d) P. Gütlich, Y. Garcia and H. A. Goodwin, *Chem. Soc. Rev.*, **29**, 419 (2000).
8 P. Gütlich, A. Hauser, and H Spiering, *Angew. Chem., Int. Ed. Engl.*, **33**, 2024 (1994).
9 N. Sakagami, M. Nakahanada, K. Ino, A. Hioki, and S. Kaizai, *Inorg. Chem.*, **35**, 683 (1996).
10 N. Sakagami, A. Hioki, M. Teramoto, A. Fuyuhiro, and S. Kaizaki, *Inorg. Chem.*, **39**, 5717 (2000).
11 O. Kahn, Y. Journaux, and C. Mathoniere , in "Magnetism: A Supramolecular Function," ed. by O. Kahn, Netherland, Kluwer Academic (1996), p.531.
12 O. Kahn and E. Codjovi, *Philos. Trans. R. Soc. Lond. A*, **354**, 359 (1996).
13 Y. Garcia, O. Kahn, L. Rabardel, B. Chansou, L. Salmon, and J. P. Tuchagues, *Inorg. Chem.*, **38**, 4663 (1999).
14 P. J. van Koningsbruggen, Y. Garcia, O. Kahn, L. Fournès, H. Kooijman, A. L. Spek, J. G. Haasnoot, J. Moscovici, K. Provost, A. Michalowicz, F. Renz, and P. Gütlich, *Inorg. Chem.*, **39**, 1891 (2000).
15 a) J-A. Real, H. Bolvin, A. Bousseksou, A. Dworkin, O. Kahn, F. Varret, and J. Zarembowitch, *J. Am. Chem. Soc.*, **114**, 4650 (1992). b) J-F. Létard, J-A. Real, N. Moliner, A. B. Gasper, L. Capes, O. Cador, and O. Kahn, *J. Am. Chem. Soc.*, **121**, 10630 (1999).
16 a) H. A. Goodwin and F. Lions, *J. Am. Chem. Soc.*, **82**, 5021 (1960). b) M. Michelsen, *Acta Chem. Scand.*, **A31**, 429 (1977).
17 P. W. Ball and A. B. Blake, *J. Chem. Soc. A*, **1969**, 1415.
18 A. Uehara, E. Kyuno, and R. Tsuchiya, *Bull. Chem. Soc. Jpn.*, **40**, 2317 (1967).
19 a) D. F. Evans, *J. Chem. Soc.*, **1959**, 2003. b) C. Piguet, *J. Chem. Educ.*, **74**, 815 (1997).
20 T. Fujihara, A. Fuyuhiro, and S. Kaizaki, *J. Chem. Soc., Dalton Trans.*, **1995**, 1813.
21 H. G. Visser, W. Purcell, and S. S. Basson, *Polyhedron*, **18**, 2795 (1999).
22 a) Y. Yamamoto and Y. Shimura, *Bull. Chem. Soc. Jpn.*, **54**, 2934 (1981). b) Y. Yamamoto, Y. Hata, and Y. Shimura, *Chem. Lett.*, **1981**, 1559.
23 M. A. Collins, D. J. Hodgson, K. Michelsen, and D. K. Towle, *J. Chem. Soc., Chem. Commun.*, **1987**, 1659.
24 C. H. Görbitz and M. C. Etter, *J. Chem. Soc., Perkin Trans. 2*, **1992**, 131.
25 a) J. Casabó, J. Pons, K. S. Siddiqi, F. Teixidor, E. Molins, and C. Miravitlles, *J. Chem. Soc., Dalton Trans.*, **1989**, 1401. b) J.

Pons, X. Lopez, J. Casabó, and F. Teixidor, A. Caubet, J. Ruis, and C. Miravitles, *Inorg. Chim. Acta*, **195**, 61 (1992). c) M. Munakata, P. L. Wu, M. Yamamoto, T. Kuroda-Sawa, M. Maekawa, S. Kawata, and S. Kitagawa, *J. Chem. Soc., Dalton Trans*., **1995**, 4099.

26 a) N. Koine, R. Bianchini and J. I. Legg, *Inorg. Chem*., **25**, 2835 (1988). b) C. A. Green, N. Koine, J. I. Legg and R. D. willet, *Inorg. Chim. Acta*, **176**, 87 (1990).

27 A. Uehara, E. Kyuno, and R. Tsuchiya, *Bull. Chem. Soc. Jpn*., **40**, 2332 (1967).

28 L. J. Wilson, D. Georges, and M. A. Hoselton, *Inorg. Chem*., **14**, 2968 (1975).

29 N. Suemura, M. Ohama, and S. Kaizaki, *Chem. Commun*., **2001**, 1538.